Communications in Computational Chemistry
Commun. Comput. Chem., Vol. 1, No. 1, 24–28
doi: 10.4208/cicc.2025.56.01

Regular Article

Effect of Molecule Coverage on Nitric Oxide Reduction Reaction on Cu(111)

Haoran Li, Ying Dai,* Baibiao Huang and Wei Wei*

School of Chemistry and Chemical Engineering, Shandong University, Jinan, 250010, People's Republic of China.

*Corresponding author: daiy60@sdu.edu.cn, weiw@sdu.edu.cn

Received on 5 March 2025; Accepted on 26 March 2025

Abstract

Electrochemical nitrogen oxide reduction reaction (NORR) can simultaneously remove atmospheric pollutant NO and produce the important chemical ammonia (NH_3), which, therefore, has garnered significant attention. However, the effect of molecule coverage on the catalyst surface on electrocatalytic activity is less discussed. In combination with atomic *ab initio* thermodynamics and first-principles calculations, the relationship between the NO coverage and catalytic NORR activity on Cu(111) is unraveled in this work. Results indicate that the adsorption stability and the limiting potential (U_L) of NORR on Cu(111) is closely related to NO coverage. In the case of standard conditions (1 atm, 300 K), NO adsorption with a coverage of 1/4 monolayer (ML) is the most stable configuration, though the corresponding U_L (0.34 V) is higher than those of 1/9 (0.29 V) and 1/16 ML (0.29 V) adsorption while significantly lower than that of 1 ML (0.78 V). Therefore, our study provides insights into the role of temperature, pressure, and molecule coverage in electrochemical reactions.

Key words: NORR, Cu(111), molecule coverage, first-principles calculations.

1. Introduction

Nitric oxide (NO) is a major atmospheric pollutant. Excessive emission of NO contributes to environmental issues including acid rain, photochemical smog, and global warming, all of which not only cause significant disruptions to human life but also pose substantial threats to public health and survival [1–6]. To address this issue, various denitrification methods have been proposed, with selective catalytic reduction (SCR) being the most widely utilized technology. Through SCR, NO can be converted into harmless nitrogen (N_2) gas and released into the atmosphere [7]. However, SCR presents several challenges including high consumption of expensive reactants and excessive energy requirements, making it economically unfeasible and environmentally unsustainable [8–11].

Ammonia (NH_3) is one of the most important chemicals in industry, with widespread applications in the production of explosives, synthetic fibers, fertilizers, and pharmaceuticals. Currently, NH_3 production in industry primarily relies on the Haber–Bosch process, which requires harsh conditions of high temperature and high pressure, accompanied by substantial energy consumption and the release of significant amounts of greenhouse gases [12–15]. In order to overcome these drawbacks, electrochemical N_2 reduction reaction (NRR) has recently garnered intensive interest. NRR occurs under mild conditions and does not generate large amounts of polluting gases, manifesting itself as a promising alternative to the Haber–Bosch technology and attracting significant attention [16,17]. However, NRR faces two significant challenges: (1) low catalytic activity due to the chemical inertness of N_2, and (2) low Faradaic efficiency (FE) because of the "'latex competing hydrogen evolution reaction (HER). Therefore, there is an urgent need to explore sustainable and environmentally friendly alternatives for efficient NH_3 production.

The concept of directly electrochemically reducing NO to simultaneously remove NO and synthesize NH_3 has been put forward [18–20]. This approach has quickly gained extensive attention as NO exhibits higher chemical reactivity than N_2, which endows the NO reduction reaction (NORR) better activity and selectivity compared to NRR. Experimental and theoretical studies have reported various electrocatalysts for NORR, such as Pt(111) [21], defective hexagonal boron nitride [22], as well as a CoN_4 moiety [23]. In particular, Cu(111) was demonstrated to have relatively high catalytic NORR activity and excellent

NH_3 selectivity, by investigating the adsorption free energy of NORR intermediates on different transition metals [18]. It should be emphasized that, for NORR, N–N coupling under high NO concentrations will lead to the formation of byproducts such as N_2O (with a global warming potential 298 times greater than CO_2) and N_2. It was found that, additionally, the generation of single N products (NH_3) on Cu(111) is favored at low NO coverages [24]. It therefore can be concluded that the electrochemical reaction and the catalytic NORR activity on Cu(111) is in close relation with the molecule coverage on the catalyst surface. Unraveling this relationship is of importance for optimizing the activity and selectivity and helps further understanding the NORR mechanism. However, a comprehensive study on the effect of NO coverage on NORR is missing.

In this work, based on the atomic *ab initio* thermodynamics in conjunction with first-principles calculations, we find that the NO molecular coverage on Cu(111) affects the catalytic NORR activity and there is a competition between the stability of the adsorption structure and the NORR limiting potential (U_L). In the case of high coverage of 1 monolayer (ML), intermolecular repulsion inhibits NO activation, resulting in a high energy barrier of 0.78 eV for the potential-determining step (PDS). It is of interest to see that the U_L decreases to 0.34, 0.29, and 0.29 V as the NO coverage decreases to 1/4, 1/9, and 1/16 ML, respectively. It should be emphasized that the adsorption structure with a 1/4 ML NO coverage is the most stable one under standard conditions (1 atm, 300 K), though it does not provide the optimum catalytic NORR activity. In this view, therefore, our results provide new insights into the effect of molecular coverage on the catalytic activity in electrochemical reactions.

2. Calculation Methods

In this work, the first-principles calculations based on spin-polarized density functional theory (DFT) were performed by using the Vienna *ab initio* simulation package (VASP) [25,26]. In order to describe the core–valence interactions, the projector-augmented wave (PAW) method [27] was used with a cutoff energy of 500 eV for the plane-wave basis set. In the framework of the generalized gradient approximation (GGA), the Perdew–Burke–Ernzerhof (PBE) scheme [28–30] was applied for the exchange–correlation functional. The convergence criteria for energy and residual force were set to 10^{-5} eV and 0.01 eV/Å, respectively, and a Monkhorst–Pack k-point mesh of $3\times3\times1$ was used for structure optimization and total energy calculation. To account for the van der Waals (vdW) interactions between the catalyst and NORR intermediates were described by employing the DFT–D2 scheme [31]. A Cu(111) surface was modeled by a slab, and a vacuum layer of 20 Å along the z direction was added to avoid interactions between periodic images.

In light of the atomic *ab initio* thermodynamics, the surface free energy γ can be employed to determine the stability of a surface in contact with a gas-phase reservoir, which is defined as

$$\gamma(T,\{p_{NO}\}) = \frac{1}{A}\Big[G^{surf} - n_{Cu}\mu_{Cu}^{bulk} - n_{NO}\mu_{NO}^{gas}(T,p_{NO})\Big],$$

where G^{surf} is the Gibbs free energy of the solid exposing the surface, A is the surface area, and μ_{Cu}^{bulk} and μ_{NO}^{gas} are the chemical potentials of bulk Cu and gaseous NO, respectively. To evaluate the stability of NO adsorption on Cu(111), the Gibbs free energy of adsorption ΔG^{ads} was calculated, which can be defined as [32,33]

$$\begin{aligned}\Delta G^{ads}(\Delta\mu_{NO}) =& \gamma_{Cu(111)} - \gamma_{NO/Cu(111)}\\ =& -\frac{1}{A}\Big[G^{surf}_{NO/Cu(111)} - G^{surf}_{Cu(111)}\\ & - \Delta n_{Cu}\mu^{bulk}_{Cu} - n_{NO}\left(E^{tot}_{NO} + \Delta\mu_{NO}\right)\Big]\\ \approx& -\frac{1}{A}\widetilde{E}^{bind}_{NO/Cu(111)} + \frac{n_{NO}}{A}\Delta\mu_{NO}\end{aligned}$$

where $G^{surf}_{NO/Cu}$ and $G^{surf}_{Cu(111)}$ are the Gibbs free energies of the Cu(111) surface with n_{NO} adsorbed NO molecules and the clean Cu(111) surface, respectively. In particular, the chemical potential of NO is composed of its total energy part and the temperature- and pressure-dependent term, that is,

$$\mu_{NO} = E^{tot}_{NO} + \Delta\mu_{NO}(T,p).$$

It has been confirmed that the difference in Gibbs free energies between the clean and the NO-adsorbed surfaces can be obtained from DFT results [34,35].

According to the computational hydrogen electrode (CHE) model proposed by Nørskov *et al.* [36], the Gibbs free energy change for each NORR step is determined by

$$\Delta G = \Delta E + \Delta E_{ZPE} - T\Delta S,$$

where ΔE is the reaction energy of each elementary step, ΔE_{ZPE} is the zero-point energy correction, and ΔS is the entropy change at room temperature (298.15 K). In an O-distal reaction pathway, the NORR proceeds stepwise as follows:

$$\begin{aligned}&NO(g) + * \rightarrow *NO,\\ &*NO + H^+ + e^- \rightarrow *NOH,\\ &*NOH + H^+ + e^- \rightarrow *N + H_2O(g),\\ &*N + H^+ + e^- \rightarrow *NH,\\ &*NH + H^+ + e^- \rightarrow *NH_2,\\ &*NH_2 + H^+ + e^- \rightarrow *NH_3.\end{aligned}$$

3. Results and discussion

It is well known that the adsorption and activation of NO is both the first and most crucial step in the NORR process, essential for the entire electrocatalytic reaction. In other words, sufficient NO adsorption strength is required, and efficient NO activation facilitates a thermodynamically easier initial protonation step. It has been demonstrated that the NO molecule on Cu(111) prefers to adsorb at the CuCuCu hollow site among the possible NO adsorption sites (Cu site, Cu–Cu bridge site, and CuCuCu hollow site) in a N-end configuration [37]. On Cu(111), further studies have shown that the NORR pathway is confirmed to follow the O-distal pattern, as illustrated in Figure 1a. In this reaction pathway, $H^+ + e^-$ first attacks the distal O atom of NO, resulting in the formation of an H_2O molecule. Subsequently, the coupled $H^+ + e^-$ continues to attack the remaining N atom, eventually producing an NH_3 molecule, which then detaches from the catalyst surface. It is important to note that the generation of byproducts other than NH_3 is a significant challenge for the NORR process. In particular, NO adsorption at high coverage

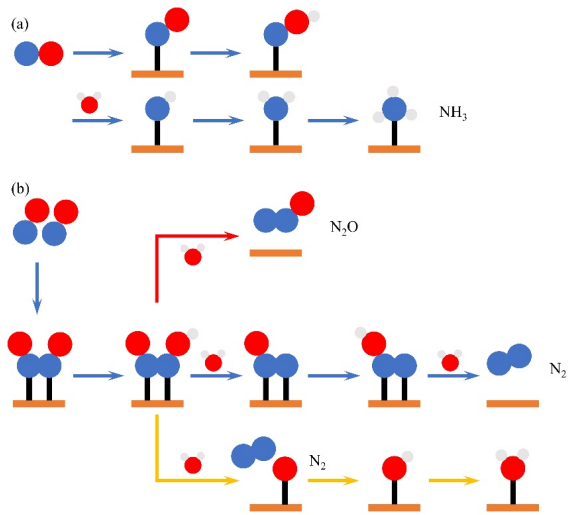

Figure 1. (a) Reaction pathway of electrocatalytic NORR toward NH_3 formation in O-distal pattern. (b) Possible reaction pathways for synthesizing N–N coupled products (N_2 and N_2O) with high NO adsorption coverage. White, blue and red spheres indicate H, N and O atoms, respectively.

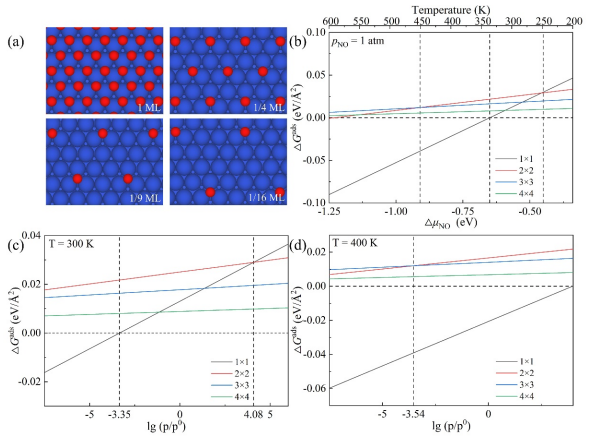

Figure 2. (a) Top views of NO adsorption on Cu(111) with different coverages. Blue and red balls represent Cu and O atoms, respectively. (b) Gibbs free energy ΔG^{ads} as a function of $\Delta\mu_{NO}$ for NO adsorption on Cu(111) under standard atmospheric pressure. Gibbs free energy ΔG^{ads} as a function of $\log(p/p^0)$ for NO adsorption on Cu(111) at (c) 300 K and (d) 500 K. In (b)–(d), curves in different color stands for results based on different Cu(111) supercells, *i.e.*, different NO coverages.

leads to a substantial possibility for the formation of N–N coupled compounds, which ultimately yield byproducts such as N_2 and N_2O [38]. In this view, the Faradaic efficiency of NH_3 production is severely reduced. In Figure 1b, possible pathways for the electrochemical formation of N–N coupled byproducts (N_2O and N_2) on Cu(111) are schematically illustrated.

To simulate different NO coverages, Cu(111) supercells of 1×1 (with a surface lattice parameter of approximately 2.58 Å, 2 × 2, 3 × 3, and 4 × 4 are considered. In the case of 1 × 1 Cu(111), one NO molecule adsorption on the surface corresponds to a coverage of 1 ML, and thus 1/4, 1/9, and 1/16 ML for the 2 × 2, 3 × 3, and 4 × 4 counterparts, respectively. In Figure 2a, optimized adsorption configurations of NO on Cu(111) are shown. It can be found that, at different coverages, the NO molecule remains the N-end adsorption configuration over the Cu–Cu–Cu hollow site. It should be pointed out that, however, the NO bond lengths differ as NO coverage decreases, which can be explained by the reduced inter-molecule repulsive interactions when the coverage decreases. In particular, the N–O bond length turns out to be 1.197, 1.220, 1.222, and 1.227 Å for 1, 1/4, 1/9, and 1/16 ML, respectively. In comparison to the NO bond length of 1.169 Å in the gas phase, the stretched bond length on Cu(111) indicates that the molecule is sufficiently activated, which is crucial for the subsequent NORR. In accordance with the Sabatier principle, moderate NO adsorption is in favor of NORR; either too strong or too weak adsorption strength can degrade the catalytic activity (insufficient activation or arduous desorption). It appears that low coverage signifies high NO activation and thus high catalytic NORR activity, while adsorption of low NO coverage may not be stable under standard conditions. In this view, the effect of NO coverage on NORR should be further discussed, aiming at providing an insight into the correlation between structure stability and catalytic activity.

In order to evaluate the stability of NO adsorption of different coverages on Cu(111), adsorption Gibbs free energy (ΔG^{ads}) of these configurations are calculated and compared with the surface free energy of clean Cu(111). In accordance to the definition, $\Delta G^{ads} > 0$ implies that the structure is stable upon adsorption, while a negative value means that the molecule cannot be adsorbed on the catalyst surface. In Figure 2b, Gibbs free energy diagram of NO adsorption on Cu(111) is presented for cases with different molecule coverages, with the gas pressure fixed at one standard atmosphere ($p_{NO} = 1$ atm). It is evident that the adsorption Gibbs free energy of NO exhibits a linear dependence on temperature (or NO chemical potential) and, naturally, the adsorption on Cu(111) turns out to be unstable as temperature increases. In respect to the 1 ML NO coverage, inter-molecular interactions lead to instability of the adsorption structure and the Gibbs free energy for NO adsorption is more sensitive to temperature compared to those of low coverages. It can be observed that the stability for NO adsorption with a coverage of 1 ML decreases rapidly as temperature increases, and the molecule will desorb from the surface when the temperature achieves 340 K. It should be noted that 1 ML NO adsorption will become the most stable configuration among all the coverages of consideration only when the temperature is lower than 247 K (corresponding to a chemical potential of $\Delta\mu_{NO} = -0.45$ eV). It therefore is an indication that extremely high coverage of NO adsorption (1 ML) is not favored on Cu(111), which is consistent with experimental observations [24]. It is of interest that, alternatively, NO adsorption with a molecule coverage of 1/4 ML is the most stable pattern over a large temperature range (from 247 K to 450 K). In case the temperature is elevated, naturally, NO adsorption of low coverages turns out to be stable; for instance, 1/9 ML coverage is the most favored one as the temperature is higher than 450 K. It can be concluded that there should be an optimum match between NO adsorption coverage and catalytic NORR activity upon Cu(111) at standard conditions.

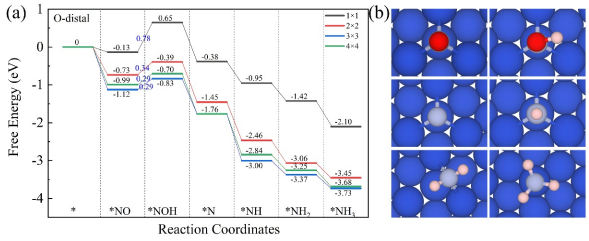

Figure 3. (a) Free energy diagram for NORR on Cu(111) supercells of consideration (corresponding to different NO coverages). Numbers in blue are the U_L. (b) Stable adsorption configurations of the key intermediates for NORR on Cu(111). Blue, gray, red and pink spheres represent Cu, N, O and H atoms, respectively.

In addition to temperature, the influence of gas pressure on NO adsorption Gibbs free energy should also be considered. In Figure 2c, Gibbs free energies for NO adsorption of different coverages on Cu(111) are compared at room temperature (300 K). It can be found that high molecule coverage (1 ML) is preferred only when $\lg(p/p^0) > 4.08$, and NO desorbs from the catalyst surface as $\lg(p/p^0) < -3.35$. In consistent with the above discussion, 1/4 coverage dominates the NO adsorption on Cu(111). In Figure 2d, Gibbs free energy of NO adsorption as a function of gas pressure is also presented at higher temperature, *i.e.*, 400 K, to explore the variation trend of the stability of the NO/Cu(111) structures. It can be seen that the stability for NO adsorption on Cu(111) deteriorates, as temperature increases. In this case (at 400 K), coverage of 1/4 ML remains primary as $\lg(p/p^0) > -3.54$, and the surface prefers low NO coverage (1/9 ML) when $\lg(p/p^0) < -3.54$.

In Figure 3a, free energy diagrams for the NORR process on Cu(111) under different NO coverages are presented, and the optimized intermediate (*i.e.*, *NO, *NOH, *N, *NH, *NH_2, and *NH_3) adsorption configurations are provided in Figure 3b. It is of interest to see that the PDS for the NORR on Cu(111) with different molecule coverages remains the first hydrogenation step (*NO + H^+ + e^- → *NOH), where a thermodynamic energy barrier is encountered. In subsequent steps, the *NOH combines with H^+ + e^- to form a free H_2O molecule, and the remaining *N will continue to be reduced spontaneously to *NH, *NH_2 and *NH_3. It obviously shows that the energy barrier encountered during the reaction decreases with varying NO coverage, though the PDS remains the first electrochemical reaction step. In particular, the U_L for the NORR on 1 × 1 Cu(111) (1 ML NO coverage) is as large as 0.78 V, signifying an inferior catalytic NORR activity. In case the NO coverage decreases to 1/4, 1/9 and 1/16 ML, the U_L for NORR on Cu(111) decreases gradually to 0.34, 0.29 and 0.29 V, respectively. In consideration of both the adsorption stability and activity, NO coverage of 1/4 ML is more preferred for electrocatalytic NORR on Cu(111) (with U_L being 0.34 V). It should be emphasized that tuning the coordination microenvironment and the local electronic structure by, for instance, *p*-block atom doping on surface can probably eliminate the thermodynamic energy barrier in the first hydrogenation step of the NORR on Cu(111).

4. Conclusion

In summary, we demonstrated that the NO molecular coverage is directly related to the catalytic NORR activity on Cu(111) by the first-principles calculations in combination with atomic *ab initio* thermodynamics. In particular, NO activation and the NORR U_L differ with varying molecule coverage, which can be attributed to the reduced inter-molecular repulsive interactions as the coverage decreases. It can be found that 1/4 ML NO adsorption is the most stable configuration under standard conditions (1 atm, 300 K), with the NORR U_L being 0.34 V. In comparison to the metastable 1/9 (U_L = 0.29 V) and 1/16 ML (U_L = 0.29 V) NO adsorption, 1/4 ML NO adsorption obviously does not correspond to the optimum catalytic NORR activity. In this view, our work conclusively confirms the effect of NO molecular coverage on the NORR on Cu(111), providing new insights into the relationship between temperature, pressure and electrocatalytic activity and highlighting the crucial role of molecular coverage in catalyst performance.

Acknowledgments

This work is supported by National Natural Science Foundation of China (52272223).

References

[1] Ren Z., Zhang H., Wang S., Huang B., Dai Y., Wei W., Nitric oxide reduction reaction for efficient ammonia synthesis on topological nodal-line semimetal Cu_2Si monolayer. *J. Mater. Chem. A*, **10** (2022), 8568–8577.

[2] Qian H., Xu S., Cao J., Ren F., Wei W., Meng J., Wu L., Air pollution reduction and climate co-benefits in China's industries. *Nat. Sustain.*, **4** (2021), 417–425.

[3] Li K., Jacob D. J., Liao H., Zhu J., Shah V. S., Shen L., Bates K. H., Zhang Q., Zhai S., A two-pollutant strategy for improving ozone and particulate air quality in China. *Nat. Geosci.*, **12** (2019), 906–910.

[4] Meng D., Zhan W., Guo Y., Guo Y., Wang L., Lu G., A highly effective catalyst of Sm-MnOx for the NH_3-SCR of NO_x at low temperature: promotional role of Sm and its catalytic performance. *ACS Catal.*, **5** (2015), 5973–5983.

[5] Wu Q., Wang H., Shen S., Huang B., Dai Y., Ma Y., Efficient nitric oxide reduction to ammonia on a metal-free electrocatalyst. *J. Mater. Chem. A*, **9** (2021), 5434–5441.

[6] Lee T., Bai H., Low temperature selective catalytic reduction of NO_x with NH_3 over Mn-based catalyst: a review. *AIMS Environ. Sci.*, **3** (2016), 261–289.

[7] Koebel M., Madia G., Elsener M., Selective catalytic reduction of NO and NO_2 at low temperatures. *Catal. Today*, **73** (2002), 239–247.

[8] Zhang R., Liu N., Lei Z., Chen B., Selective transformation of various nitrogen-containing exhaust gases toward N_2 over zeolite catalysts. *Chem. Rev.*, **116** (2016), 3658–3721.

[9] Burch R., Breen J. P., Meunier F. C., A review of the selective reduction of NO_x with hydrocarbons under lean-burn conditions with non-zeolitic oxide and platinum group metal catalysts. *Appl. Catal. B*, **39** (2002), 283–303.

[10] Forzatti P., Present status and perspectives in de-NO_x SCR catalysis. *Appl. Catal. A Gen.*, **222** (2001), 221–236.

[11] Kim C. H., Qi G., Dahlberg K., Li W., Strontium-doped perovskites rival platinum catalysts for treating NO_x in simulated diesel exhaust. *Science*, **327** (2010), 1624–1627.

[12] Lv X., Wei W., Huang B., Dai Y., Frauenheim T., High-throughput screening of synergistic transition metal dual-atom catalysts for efficient nitrogen fixation. *Nano Lett.*, **21** (2021), 1871–1878.

[13] Ma Z., Xiao C., Cui Z., Du W., Li Q., Sa R., Sun C., Defective Fe_3GeTe_2 monolayer as a promising electrocatalyst for spontaneous nitrogen reduction reaction. *J. Mater. Chem. A*, **9** (2021), 6945–6954.

[14] Chen Z., Yan J.-M., Jiang Q., Single or double: which is the altar of atomic catalysts for nitrogen reduction reaction? *Small Methods*, **3** (2019), 1800291.

[15] Liu Y., Deng P., Wu R., Zhang X., Sun C., Li H., Oxygen vacancies for promoting the electrochemical nitrogen reduction reaction. *J. Mater. Chem. A*, **9** (2021), 6694–6709.

[16] Jasin Arachchige L., Xu Y., Dai Z., Zhang X., Wang F., Sun C., Double transition metal atoms anchored on graphdiyne as promising catalyst for electrochemical nitrogen reduction reaction. *J. Mater. Sci. Technol.*, **77** (2021), 244–251.

[17] Li L., Wang X., Guo H., Yao G., Yu H., Tian Z., Li B., Chen L., Theoretical screening of single transition metal atoms embedded in MXene defects as superior electrocatalyst of nitrogen reduction reaction. *Small Methods*, **3** (2019), 1900337.

[18] Long J., Chen S., Zhang Y., Guo C., Fu X., Deng D., Xiao J., Direct electrochemical ammonia synthesis from nitric oxide. *Angew. Chem. Int. Ed.*, **59** (2020), 9711–9718.

[19] Shi J., Wang C., Yang R., Chen F., Meng N., Yu Y., Zhang B., Promoting nitric oxide electroreduction to ammonia over electron-rich Cu modulated by Ru doping. *Sci. China Chem.*, **64** (2021), 1493–1497.

[20] Long J., Guo C., Fu X., Jing H., Qin G., Li H., Xiao J., Unveiling potential dependence in NO electroreduction to ammonia. *J. Phys. Chem. Lett.*, **12** (2021), 6988–6995.

[21] Clayborne A., Chun H.-J., Rankin R. B., Greeley J., Elucidation of pathways for NO electroreduction on Pt(111) from first principles. *Angew. Chem. Int. Ed.*, **54** (2015), 8255–8258.

[22] Sun P., Wang W., Zhao X., Dang J., Defective h-BN sheet embedded atomic metals as highly active and selective electrocatalysts for NH_3 fabrication via NO reduction. *Phys. Chem. Chem. Phys.*, **22** (2020), 22627–22634.

[23] Wang Z., Zhao J., Wang J., Cabrera C. R., Chen Z., A Co-N_4 moiety embedded into graphene as an efficient single-atom-catalyst for NO electrochemical reduction: a computational study. *J. Mater. Chem. A*, **6** (2018), 7547–7556.

[24] Ko B. H., Hasa B., Shin H., Zhao Y., Jiao F., Electrochemical reduction of gaseous nitrogen oxides on transition metals at ambient conditions. *J. Am. Chem. Soc.*, **144** (2022), 1258–1266.

[25] Kresse G., Furthmüller J., Efficient iterative schemes for ab initio total-energy calculations using a plane-wave basis set. *Phys. Rev. B*, **54** (1996), 11169–11186.

[26] Kresse G., Joubert D., From ultrasoft pseudopotentials to the projector augmented wave method. *Phys. Rev. B*, **59** (1999), 1758–1775.

[27] Perdew J. P., Wang Y., Accurate and simple analytic representation of the electron-gas correlation energy. *Phys. Rev. B*, **45** (1992), 13244–13249.

[28] Becke A. D., Density-functional exchange-energy approximation with correct asymptotic behavior. *Phys. Rev. A*, **38** (1988), 3098.

[29] Perdew J. P., Burke K., Ernzerhof M., Generalized gradient approximation made simple. *Phys. Rev. Lett.*, **78** (1996), 1396.

[30] Lee C., Yang W., Parr R. G., Development of the Colle-Salvetti correlation-energy formula into a functional of the electron density. *Phys. Rev. B*, **37** (1988), 785.

[31] Liechtenstein A. I., Anisimov V. I., Zaanen J., Density-functional theory and strong interactions: orbital ordering in Mott-Hubbard insulators. *Phys. Rev. B*, **52** (1995), R5467–R5470.

[32] Li W., Stampfl C., Scheffler M., Why is a noble metal catalytically active? The role of the O-Ag interaction in the function of silver as an oxidation catalyst. *Phys. Rev. Lett.*, **90** (2003), 256102.

[33] Reuter K., Scheffler M., Oxide formation at the surface of late 4d transition metals: insights from first-principles atomistic thermodynamics. *Appl. Phys. A*, **78** (2004), 793.

[34] Reuter K., Scheffler M., Composition, structure, and stability of RuO_2(110) as a function of oxygen pressure. *Phys. Rev. B*, **65** (2001), 035406.

[35] Reuter K., Scheffler M., Composition and structure of the RuO_2(110) surface in an O_2 and CO environment: implications for the catalytic formation of CO_2. *Phys. Rev. B*, **68** (2003), 045407.

[36] Nørskov J. K., Rossmeisl J., Logadottir A., Lindqvist L., Kitchin J. R., Bligaard T., Jónsson H., Origin of the overpotential for oxygen reduction at a fuel-cell cathode. *J. Phys. Chem. B*, **108** (2004), 17886–17892.

[37] Wan H., Bagger A., Rossmeisl J., Electrochemical nitric oxide reduction on metal surfaces. *Angew. Chem. Int. Ed.*, **60** (2021), 21966–21972.